# Expression and light-dependent translocation of β-arrestin in the visual system of the terrestrial slug *Limax valentianus*

Ryota Matsuo[1]*, Yuka Takatori[1], Shun Hamada[2], Mitsumasa Koyanagi[3], and Yuko Matsuo[1]

[1]Department of Environmental Sciences, International College of Arts and Sciences, Fukuoka Women's University

[2]Department of Nutrition and Health Sciences, International College of Arts and Sciences, Fukuoka Women's University

[3]Department of Biology and Geosciences, Graduate School of Science, Osaka City University

Keywords: β-arrestin, translocation, optic nerve, rhodopsin, retina, gastropod

*Address all correspondence to: Ryota MATSUO, Ph.D.

Laboratory of Neurobiology,

International College of Arts and Sciences, Fukuoka Women's University,

1-1-1 Kasumigaoka, Higashi-ku, Fukuoka 813-8529, Japan

Phone: +81-92-692-3119

Fax: +81-92-661-2420

E-mail: matsuor@fwu.ac.jp

## SUMMARY STATEMENT

Immunostaining of β-arrestin revealed its light-dependent translocation in the photoreceptors of a terrestrial slug, and also showed the utility of β-arrestin as a molecular marker of optic nerves.

## ABSTRACT

Vertebrates, cephalopods, and arthropods are equipped with eyes having the highest spatiotemporal resolution among the animal phyla. In parallel, it is only the animals in these three phyla that have visual arrestin specialized for the termination of visual signaling triggered by opsin, in addition to ubiquitously expressed β-arrestin that serves in terminating general G protein-coupled receptor signaling. Indeed, visual arrestin in *Drosophila* and rodents translocates to the opsin-rich subcellular region in response to light to reduce the overall sensitivity of photoreceptors in an illuminated environment (i.e. light adaptation). We thus hypothesized that visual arrestin has taken over the role of β-arrestin in those animals having an eye with high spatiotemporal resolution during evolution. If this is true, it is expected that β-arrestin plays a role similar to visual arrestin in those animals having low resolution eyes. In the present study, we focused on the terrestrial mollusk *Limax*, a species related to cephalopods but has only β-arrestin, and generated antibody against β-arrestin. We found that β-arrestin is highly expressed in photosensory neurons, and translocates into the microvilli of the rhabdomere within 30 min in response to short wavelength light (400 nm), to which the eye of *Limax* exhibits a robust response. These observations suggest that β-arrestin functions in the visual system of those animals that do not have visual arrestin. We also exploited anti-β-arrestin antibody to visualize the optic nerve projecting to the brain, and demonstrated its usefulness for tracing a visual ascending pathway.

## INTRODUCTION

Most of the metazoan animal species have eyes as a sensory organ specialized for the detection of ambient light. The evolution of eyes has been discussed in terms of their structural and functional characteristics, such as the directionality of photoreception, membrane stacking, integration time, the functionality of the lens, and so on (Land and Nilsson, 2012; Nilsson, 2013). Acquisition and refinement of these elements resulted in the development of eyes with high performance.

Among the animal phyla, vertebrates, cephalopods, and arthropods have acquired the most exquisite eyes with high temporal and spatial resolution (classified as "class IV" by Nilsson (2013)). Are there any molecular bases for the exquisiteness of the eyes of the animals in these three phyla? Regulation of the lifetime of rhodopsin signaling is one of the determinants of the temporal resolution of eyes. Arrestin is thought to play an important role in this process because it takes part in the termination of rhodopsin signaling (Arshavsky, 2003; Calvert et al., 2006). Here we have noticed that the photoreceptors of the animals belonging to these three animal phyla possess the arrestin specialized for vision (visual arrestin) in addition to β-arrestin as a signaling component of phototransduction (Gurevich and Gurevich, 2006; Yoshida et al., 2015). Arrestin family proteins function in terminating G protein-coupled receptor (GPCR) signaling by binding the intracellular domain of the GPCR, thereby sterically blocking further G protein activation. Of these, β-arrestin has a clathrin-binding domain in its C-terminus, and is ubiquitously expressed serving as a terminator for all GPCR signaling. On the other hand, visual arrestin is devoid of a clathrin-binding domain, and is specialized for the termination of opsin signaling in photoreceptors (Gurevich and Gurevich, 2006). If the presence of visual arrestin is a key factor for high performance of the "classIV" eyes, it must be subserving the high temporal resolution by promoting rapid turnover of activation/inactivation of rhodopsin signaling.

If the above mentioned parallelism is actually meaningful, it is expected that the animals with less-developed eyes should cope with living tasks using only β-arrestin. In the present study, we focused on the gastropod *Limax*, because it is evolutionarily related to cephalopods but considered to have less elaborated eyes, and seems to live

lives with less demanding of rapidity. According to Nilsson (2013), the eye of gastropods is categorized as "class III" (having a medium spatiotemporal resolution) due to the small number of photoreceptors and under-focused lenses. First, we confirmed that the eye of *Limax* has a simple structure, and that *Limax* has β-arrestin but is devoid of visual arrestin. We then analyzed the expression of β-arrestin in the eye and in other parts of the central nervous system (CNS).

Visual arrestin is known to translocate to the rhabdomeric region/outer segment of the photoreceptors in response to light in *Drosophila* and vertebrates (Broekhuyse et al., 1985; Philp et al., 1987; Kiselev et al., 2000; Nair et al., 2002; Lee et al., 2003). Such translocation serves to down-regulate the overall signaling from rhodopsins. The light-dependent translocation of arrestin, therefore, is thought to play a pivotal role in the light adaptation of the photoreceptor (Calvert et al., 2006). However, it is uncertain whether β-arrestin exhibits similar light-dependent behavior in the photoreceptors involved in vision of those animals that lack visual arrestin. We thus tested whether β-arrestin translocates to the rhabdomeric region of the photoreceptor in response to light, and analyzed its wavelength dependency by means of immunohistochemical staining.

Immunohistochemical visualization of β-arrestin is also important for tracing the flow of visual information in the brain of the slug. It has been suggested by previous studies that some of the visual information entering into the brain from an eye crosses the commissure of the cerebral ganglia, and inputs into the contralateral side of the brain (Tuchina et al., 2011; Matsuo et al., 2014b). In these studies, the visual tract was marked with neurobiotin incorporated from the cut end of the optic nerve. Such bilateral crosstalk likely enables the slug's negative phototaxis behavior through comparison of the light intensities between the bilateral eyes, thereby allowing efficient escape from a light place (Matsuo et al., 2014b). However, incorporation of neurobiotin does not necessarily mean that the optic nerve directly projects to the other side of the cerebral ganglion. This is because neurobiotin easily passes gap junctions (Hampson et al., 1992), hence the commissural nerve may be a part of neurons distinct from those projecting to the brain from an eye. Therefore, a different molecular tool is necessary. β-arrestin is a good candidate to serve this role. Indeed, the optic nerves have once been visualized by

immunohistochemical staining of this protein in planaria because β-arrestin protein is enriched in the photoreceptor cells and optic nerves in this species (Cross et al., 2015).

In the present study, we first investigated the structure of the retina of the eye of *Limax*. We then cloned the cDNAs of β-arrestin and rhodopsin from *Limax*, and raised antibody against the proteins encoded by these genes. The anatomical features of the eye were analyzed using these antibodies. We then investigated whether β-arrestin exhibits light-dependent redistribution in the photosensory neurons in a wavelength dependent-manner. Finally, anti-β-arrestin antibody was applied to visualize the optic nerve to trace the flow of visual information in the brain, as well as to monitor the re-innervation of optic nerves during tentacle regeneration after the tentacle amputation.

## MATERIALS AND METHODS

*Animals*

Terrestrial slugs *Limax valentianus* (Férussac 1822) have been maintained in our laboratory at 19ºC for at least 29 generations as a closed colony. They were fed a diet of humidified powder mixture consisting of 500 g of potato starch, 521 g of rat chow (Oriental Yeast, Tokyo, Japan), and 21 g of mixed vitamins (Oriental Yeast). The age of the slugs was between 3 to 4 months after hatching at the start of all experiments.

*Toluidine blue staining and electron microscopy*

The slug was deeply anesthetized with an injection of ice-cold $Mg^{2+}$ buffer (57.6 mmol $l^{-1}$ $MgCl_2$, 5.0 mmol $l^{-1}$ glucose, 5.0 mmol $l^{-1}$ HEPES, pH 7.0) into the body cavity, and the superior tentacle was isolated. The tentacle was fixed by immersion fixation with 2% paraformaldehyde and 2% glutaraldehyde in 0.02 mol $l^{-1}$ phosphate buffer (pH 7.3) at 4°C overnight. The tissues were rinsed, osmificated, dehydrated, and embedded in epoxy resin. Semi-thin (1 μm-thick) sections were cut on an ultramicrotome (Leica EM UC7, Leica Microsystems, Wetzler, Germany) and stained with 0.5% toluidine blue dissolved in 1% borate buffer. The images were obtained with an Eclipse E800 microscope (Nikon, Tokyo, Japan) equipped with a DXM1200F digital CCD camera (Nikon) and a ×40 (NA 0.95) objective lens. Ultrathin sections were cut on the ultramicrotome, stained with uranyl acetate and lead citrate, and examined with an electron microscope (JEM-1400plus; JEOL, Tokyo, Japan).

*Molecular cloning of arrestin cDNA*

The cDNA of arrestin was cloned by 5'-SMART rapid amplification of cDNA ends (5'-SMART-RACE, Takara, Kusatsu, Japan) and reverse transcription-PCR (RT-PCR) using template cDNAs synthesized from the RNAs derived from the brain and the tentacle. The PCR primers were designed based on the nucleotide sequence of putative

arrestin partial cDNA found in RNA-seq data of *Limax* (NCBI BioProject acc. no. PRJDB3972). The nucleotide sequences of the PCR primers were 5'-CGCCACATGGCTTGCCAGTGTCTCCAGGTG-3' and 5'-TACAGAAGCTGGGGAATTTGGTGGCAGCTC -3' for the 1st and 2nd gene specific primers, respectively in the 5'-SMART-RACE, and 5'-CACCTGGAGACACTGGCAAG-3' and 5'-TGGCAGACTCACTTGTTTAGAAAC-3' for the molecular cloning of the C-terminal region of arrestin cDNA. The obtained PCR fragments were purified using the Wizard SV Gel and PCR clean-up system (Promega, Fitchburg, WI, USA) according to the manufacturer's instructions, and then precipitated with ethanol. The termini of the concentrated PCR product was phosphorylated by T7 polynucleotide kinase, and ligated into a cloning vector pBluescriptII (Agilent Technologies, Santa Clara, CA, USA) that had undergone digestion with EcoRV followed by dephosphorylation by shrimp alkaline phosphatase (Takara). Competent *E. coli* (Dh5α) was transformed with these plasmid vectors, and the plasmids were extracted using a GenElute plasmid miniprep kit (Sigma-Aldrich, St. Louis, MO, USA). The nucleotide sequences of the plasmid inserts were confirmed using a DNA sequencer (Genetic Analyzer 3500, Applied Biosystems, Waltham, MA). The The nucleotide sequence information of *Limax* arrestin (β-arrestin) was deposited in Genbank (accession number: LC218443).

*Phylogenetic analysis*

Phylogenetic tree inference was performed as described (Koyanagi et al., 2004). Briefly, multiple alignment of the amino acid sequences of arrestins, including *Limax* β-arrestin, was carried out with the aid of XCED software (Katoh et al., 2002). A molecular phylogenetic tree was inferred by the neighbor-joining method (Saitou and Nei, 1987). Bootstrap analysis was performed based on 1000 sets of resampled sequences using Felsenstein's method (Felsenstein, 1985). The accession numbers of the sequences used for analysis were as follows: human (*Homo*) rod arrestin, NM_000541; medaka (*Oryzias*) rod arrestin-1, AB002554; medaka rod arrestin-2, AB029392; human cone arrestin, NM_004312; medaka cone arrestin, AB002555; lamprey (*Lethenteron*)visual

arrestin, AB495339; human β-arrestin-1, NM_004041; zebrafish (*Danio*) β-arrestin-1, NM_001159822; human β-arrestin-2, NM_004313; rainbow trout (*Oncorhynchus*) red blood cell arrestin, U48410; lamprey β-arrestin, AB495338; ascidian (*Ciona*) arrestin, AB052669; fruitfly (*Drosophila*) arrestin-1, NM_057333; fruitfly arrestin-2, NM_079252; octopus (*Octopus*) visual arrestin, XM_014928485; splendid squid (*Loligo*) visual arrestin, AF393635; pygmy squid (*Idiosepius*) visual arrestin, LC021441; bobtail squid (*Euprymna*) eye arrestin, EU344779; fruitfly kurtz, AF221066; nematode (*Caenorhabditis*) β-arrestin, NM_075782; oyster (*Crassostrea*) β-arrestin, XM_011435491;limpet (*Lottia*) β-arrestin, XM_009058330; scallop (*Argopecten*) Arr12, HQ695998; scallop Arr23, HQ695999; octopus β-arrestin-1-like, XM_014914803; pygmy squid β-arrestin, LC021440; nautilus (*Nautilus*) β-arrestin, LC021439; sea hare (*Aplysia*) β-arrestin-1-like, XM_013090298; slug (*Limax*) β-arrestin, LC218443.

*Expression analysis of β-arrestin by RT-PCR*

Molecular cloning of β-arrestin was performed by RT-PCR as described previously using template cDNAs synthesized from the RNAs derived from the cerebral ganglia, subesophageal ganglia, or superior tentacle (Fukunaga et al., 2006). The nucleotide sequences of the PCR primers were: 5'-CATGACTCCACTGCTGTCAAAC-3' and 5'-GTGGCTGCTCTCAAGATCCAC-3' for β-arrestin, and 5'-GCTTACCAAGCTCCGACCCTCGTGG-3' and 5'-CGTCACTACCTCCCCGTGCCGGG-3' for 18S ribosomal RNA (rRNA).

*In situ hybridization of β-arrestin and rhodopsin*

cDNA fragments of β-arrestin and rhodopsin (Genbank accession number: LC223120) were amplified by RT-PCR using the template cDNAs synthesized from the RNAs derived from the whole CNS and the superior tentacle of the slug, respectively. The nucleotide sequences of the PCR primers were 5'-CACCTGGAGACACTGGCAAG-3' and 5'-TGGCAGACTCACTTGTTTAGAAAC-3' for β-arrestin, and

5'-GCCGCAATGAGCAGGATGGAC-3' and 5'-GACTGCGTGGAGGCTGCTGC-3' for rhodopsin. The PCR fragments were ligated into a cloning vector pCRII-TOPO (Thermo Scientific, Waltham, MA, USA) according to the manufacturer's instructions. The obtained plasmid clones were used as templates for *in vitro* transcription of digoxigenin-labeled cRNA probes as described previously (Fukunaga et al., 2006). The final concentrations of antisense and sense cRNA probes were determined so that their titers were equivalent. Fresh-frozen sections (14 μm-thick) of the superior tentacles and brains were mounted onto a glass slide coated with Vectabond (Vector Laboratories, Burlingame, CA, USA). The hybridization (at 52°C) and wash were performed as described in Fukunaga et al. (2006). The hybridized cRNA probes were detected using anti-digoxigenin antibody conjugated with alkaline phosphatase (Roche Diagnostics, Basel, Switzerland). The fluorescence substrates of alkaline phosphatase were used because the tissues in the superior tentacle are intrinsically brown-colored, which made it difficult to distinguish the positive signals using a color development method. The fluorescence substrates of alkaline phosphatase (HNPP fluorescence detection set) were purchased from Roche Diagnostics, and used according to the manufacturer's instruction. The reaction was stopped by incubation of the sections with TE buffer for 10 min (10 mmol $l^{-1}$ Tris (pH8.0), 1 mmol $l^{-1}$ EDTA). The nuclei were then stained with 0.1 μg $ml^{-1}$ 4'6-diamidino-2-phenylindole (DAPI) in TE for 10 min, followed by a wash with TE buffer. The images were obtained with an Eclipse E600 microscope (Nikon) equipped with a DP70 digital CCD camera (Olympus, Tokyo, Japan) and a ×20 (NA 0.50) objective lens.

*Preparation of bacterially-expressed β-arrestin protein and generation of anti-β-arrestin antibody*

β-arrestin protein was bacterially expressed as glutathione S-transferase (GST) fusion protein using an expression vector pGEX-6P-2 (GE Healthcare, Little Chalfont, UK), and was purified essentially as described previously (Matsuo et al., 2014a). Briefly, a full open reading frame of β-arrestin was ligated into pGEX-6P-2 using BamHI and XhoI restriction sites, and competent *E. coli* (Dh5α) was transformed with this vector.

The expression of the β-arrestin fused to the C-terminus of GST was induced by 0.2 mmol l$^{-1}$ isopropyl-β-D-thiogalactopyranoside at 22°C overnight. The recombinant protein was purified using Glutathione Sepharose 4B beads (GE Healthcare) as described previously (Yamagishi et al., 2012). The fusion protein was then digested with PreScission Protease (GE Healthcare), and the GST moiety and PreScission Protease were removed using Glutathione Sepharose 4B beads. The antiserum was obtained by immunizing a rabbit with the purified recombinant β-arrestin protein, and the antibody was affinity-purified from the antiserum using the recombinant β-arrestin protein covalently attached to NHS-activated Sepharose 4 Fast Flow beads (GE Healthcare) as described previously (Matsuo et al., 2001). The concentration of the purified antibody was determined using a Pierce BCA protein assay kit (Thermo Scientific) according to the manufacturer's instructions.

*Generation of anti-rhodopsin antibody*

A rabbit was immunized with C-terminal 19 aa (VITQADVDGSYSNKAYQID) of *Limax* rhodopsin, that was conjugated to Keyhole limpet hemocyanin via cysteine residue added to the peptide's N-terminus. The antibody was purified from the antiserum using the same peptide conjugated to NHS-activated Sepharose 4 Fast Flow beads. The concentration of the purified antibody was determined using a Pierce BCA protein assay kit.

*Cell culture and transfection*

COS-7 cells were cultured on 6-well dishes in Dulbecco's Modified Eagle Medium (Thermo Scientific) supplemented with 10% fetal bovine serum (Sigma-Aldrich) at 37°C in 5% $CO_2$, 95% air. Mammalian expression vector pcDNA3.1 (Thermo Scientific) harboring a full open reading frame of β-arrestin was transfected using Lipofectamine 3000 reagent (Thermo Scientific) according to the manufacturer's instructions. Following 24 h, the cells were washed with cold PBS, and harvested by ice-cold TNE buffer that contained 10 mmol l$^{-1}$ Tris (pH7.5), 1 mmol l$^{-1}$ EDTA, 1%

(v/v) Nonidet P-40, protease inhibitor cocktail (Wako, Osaka, Japan). The protein concentration was determined using a Pierce BCA protein assay kit.

*Preparation of protein samples and western blotting*

For the samples of western blotting of β-arrestin, the brain (w/o the buccal ganglia) and the superior tentacles were isolated under anesthesia. The brain was further dissected into cerebral and subesophageal ganglia. The tissues were homogenized in ice-cold TNE buffer. For the samples of western blotting of rhodopsin, a crude membrane fraction was obtained as follows: the brain or the superior tentacle was homogenized in ice-cold buffer consisting of 10 mmol $l^{-1}$ Tris (pH8.0), 0.25 mol $l^{-1}$ sucrose, 1 mmol $l^{-1}$ EDTA, 10 mmol $l^{-1}$ β-mercaptoethanol, supplemented with protease inhibitor cocktail (Wako), followed by centrifugation at 1400 ×g for 10 min at 4°C. The supernatant was then ultracentrifuged at 100000 ×g for 60 min at 4°C, and the pellet was dissolved in TNE buffer supplemented with protease inhibitor cocktail. The protein concentrations of the homogenates were determined using a Pierce BCA protein assay kit. An equivalent volume of SDS-sample buffer (50 mmol $l^{-1}$ Tris (pH6.8), 4% SDS, 10% glycerol, 10% mercaptoethanol, 0.1% bromophenol blue) was added to the homogenates, and the mixture was boiled at 100°C. The lysates containing 3 or 7.5 μg protein were electrophoresed on a SDS-polyacrylamide (12%) gel for the blot of β-arrestin, and those containing 5 μg or protein were electrophoresed on a SDS-polyacrylamide (10%) gel for the blot of rhodopsin. The electrophoresed protein was electrically transferred to nitrocellulose membrane (GE Healthcare). The membrane was blocked with 5% skim milk in TTBS (20 mmol $l^{-1}$ Tris (pH7.5), 137 mmol $l^{-1}$ NaCl, 0.2% Tween-20) at 4°C overnight. The membrane was incubated with 0.3 μg $ml^{-1}$ anti-β-arrestin or anti-α-tubulin mouse monoclonal antibody (1:5000, clone B-5-1-2, Sigma-Aldrich) in TTBS at room temperature for 1 h, washed 3 times in TTBS, and then incubated with horseradish peroxidase-conjugated anti-rabbit IgG (for β-arrestin) or anti-mouse IgG antibody (for α-tubulin, both 1:10000, GE Healthcare) in TTBS for 50 min at room temperature. The blots were washed 3 times in TTBS, and the signals were detected using ImmunoStar LD (Wako) and LuminoGraph I (ATTO, Tokyo, Japan).

*Tentacle amputation*

To monitor the process of tentacle regeneration using anti-β-arrestin antibody, we prepared the slugs whose tentacle was surgically amputated. The left superior tentacle was amputated under anesthesia essentially as described previously (Yamagishi et al., 2008) with slight modification. Briefly, a small cut was made with microscissors on the left side of the head, and the superior tentacle (including the optic nerve) was cut at the base near the procerebrum. The left superior tentacle was then pulled out. After surgery, $300 - 400$ µl of physiological saline (70 mmol $l^{-1}$ NaCl, 2.0 mmol $l^{-1}$ KCl, 4.7 mmol $l^{-1}$ MgCl$_2$, 4.9 mmol $l^{-1}$ CaCl$_2$, 5.0 mmol $l^{-1}$ glucose, and 5.0 mmol $l^{-1}$ HEPES adjusted to pH 7.0) was injected into the body cavity to facilitate the recovery from the anesthesia.

*Immunohistochemistry*

The brain or superior tentacle was isolated as described above, and was frozen in Surgipath FSC 22 Clear Frozen Section Compound (Leica Microsystems) using liquid nitrogen. The cryostat sections (14 µm- or 6 µm-thick) were cut and mounted onto the glass slides coated with Vectabond. They were fixed in 4% paraformaldehyde/0.1% glutaraldehyde in PBS for 30 min at room temperature. To immunostain an optic nerve entering into the brain, the isolated brain was fixed in 4% paraformaldehyde in PBS by immersion fixation for 1 h followed by cryoprotection in 20% sucrose in PBS at 4°C overnight before being frozen in Surgipath FSC 22 Clear Frozen Section Compound using liquid nitrogen. The sections (14 µm-thick) were post-fixed with 5% neutralized formalin for 20 min at room temperature. They were then treated with 0.1% TritonX-100 dissolved in PBS (PBST) for 10 min. After a brief wash in PBS, the sections were blocked in blocking buffer (PBST supplemented with 2.5% goat serum and 2.5% BSA) at room temperature for 1-8 h, and then incubated with anti-β-arrestin antibody (0.3 µg ml$^{-1}$ in blocking buffer) or anti-rhodopsin antibody (0.5 µg ml$^{-1}$ in blocking buffer) at 4°C overnight. In some experiments, the primary antibody was omitted to show the absence of non-specific binding of the secondary antibody and blocking buffer was laid instead at 4°C overnight. The sections were washed three times

in PBS, followed by incubation for 50 min with a secondary antibody against rabbit IgG labeled with Alexa Fluor 488 (1:500 in blocking buffer, Life Technologies, Carlsbad, CA, USA) at room temperature. After a wash in PBS, the sections were incubated with 0.1 μg ml$^{-1}$ DAPI in PBS for 10 min, and washed again in PBS. The sections were mounted under a coverslip in Fluoromount G (SouthernBiotech, Birmingham, AL, USA). To confirm the specificity of the primary antibody, anti-β-arrestin antibody (900 μl, 0.3 μg ml$^{-1}$ in blocking buffer) was incubated with the recombinant β-arrestin protein covalently attached to NHS-activated Sepharose 4 Fast Flow beads (100 μl as a bed volume, see above) at 4°C overnight, and the supernatant was used for the primary antibody reaction. For dual staining of β-arrestin and α-tubulin, the sections were cut 6 μm-thick, and the primary antibody was a mixture of anti-β-arrestin antibody (0.3 μg ml$^{-1}$) and anti-α-tubulin mouse monoclonal antibody (1:2000, clone B-5-1-2, Sigma-Aldrich) in blocking buffer, and the secondary antibody was a mixture of anti-rabbit IgG (Alexa488-labeled, 1:500) and anti-mouse IgG (Alexa594-labeled, 1:500, Life Technologies) in blocking buffer. The fluorescence images were obtained with a microscope (Eclipse E600) equipped with a CCD camera (DP70), ×20 (NA 0.50) and ×40 (NA 0.75) objective lenses. The brightness and contrast were adjusted for some images using the software Canvas X (Deneba, Victoria, Canada), if necessary. To calculate the ratio of the mean pixel intensities between the cell body and the rhabdomeric regions, the images of 2 serial sections (14 μm-thick) almost intersecting the center of the eye were chosen. The mean pixel intensities were measured using the software Photoshop CS2 (Adobe, San Jose, CA, USA), and the ratios were calculated and then averaged between the 2 sections. The measurements were performed in 6 to 8 independent superior tentacles.

*Electroretinogram (ERG) recording*

The ERG was recorded from the surface of an isolated eye in physiological saline. A glass electrode (tip diameters of approx. 50 μm) filled with physiological saline was attached to the outer surface of the isolated eye. The signals were amplified using a differential amplifier (Model 3000, A-M Systems, Sequim, WA, USA), and were

recorded on a computer via an A/D converter (PowerLab2/26, AD Instruments, Dunedin, New Zealand). The ERG signals were low-pass filtered at 3 Hz, and the difference between the highest and lowest peaks was calculated as an ERG amplitude. Monochromatic light was delivered by a 500 W xenon arc light system (model XW-500Q, Sanso, Tokyo, Japan). The light intensity was measured by a photopower meter (model TQ8210, Advantest, Tokyo, Japan). The eye was illuminated with 6 different wavelengths (400, 440, 480, 520, 560, and 600 nm) of monochromatic light for 1 s with the 30 min intervals in between. Light of equivalent photon flux densities $(2.25 \times 10^{13}$ photons $cm^{-2}sec^{-1})$ was delivered for different wavelengths. In some experiment, 600 nm monochromatic light $(3.77 \times 10^{14}$ photons $cm^{-2}sec^{-1})$ was delivered for 2 h. Each eye sample underwent a single series of illuminations either from 400 nm to 600 nm or from 600 nm to 400 nm, and the directions were counterbalanced among all preparations. The ERG amplitude was expressed as a ratio to the maximum ERG amplitude in each preparation, and was averaged across all preparations (n = 8). All recordings were performed at 16 -24°C.

*Incorporation and staining of neurobiotin*

Neurobiotin (Vector Laboratories) was incorporated anterogradely or retrogradely from the cut end of the optic nerve of an isolated brain as described previously (Matsuo et al., 2014b). For the dual staining of β-arrestin and neurobiotin anterogradely incorporated into the brain, the brain was fixed with 4% paraformaldehyde in PBS for 1 h followed by cryoprotection in 20% sucrose in PBS at 4°C overnight. For the dual staining of FMRFamide and neurobiotin, the brain was fixed in Bouin fixative (2.9% picric acid, 8.8% formaldehyde, 4.8% acetic acid) for 1 h and was immersed in 70% ethanol for 6 h followed by cryoprotection in 20% sucrose in PBS at 4°C overnight. For the retrograde incorporation into the eye, the superior tentacle, including the eye, was fixed in 4% paraformaldehyde in PBS for 1 h at room temperature, followed by cryoprotection in 20% sucrose in PBS at 4°C overnight. The fixed tissues were frozen in Surgipath FSC 22 Clear Frozen Section Compound using liquid nitrogen. The cryostat sections (14 μm-thick) were mounted onto glass slides coated with Vectabond. The sections were

stained with Alexa594-labeled streptavidin (1:1000, Thermo Scientific) and with either of anti-β-arrestin antibody (0.3 µg ml$^{-1}$) or anti-FMRFamide antibody (1:3000, Neuromics, Northfield, MN, USA) as described previously (Matsuo et al., 2014b). The secondary antibody was anti-rabbit IgG labeled with Alexa Fluor 488 (1:500).

*Statistical analysis*

The data were statistically analyzed using a one-way ANOVA with a post hoc Scheffé test, or by a Student's *t*-test, with a significance level of $P < 0.05$. The data are expressed as the mean ± S.E..

# RESULTS

*Structure of the eye of Limax*

We first analyzed the architecture of the eye of *Limax*. Toluidine-blue staining of a semithin section revealed the elements of the eye, including the lens, rhabdomere, pigment layer, and optic nerve (Fig. 1A). The number of neurons having apical projection (AP) was not large. To further analyze the structure of the rhabdomeric region where the proteins involved in photoreception are thought to exist, an electron microscopic image was acquired (Fig. 1B). As reported previously in other pulmonates (Kataoka, 1975; Katagiri et al., 2001), an innumerable number of microvilli were evident around the AP that extrudes out from the pigment layer and contains a lot of mitochondria. To examine whether all of the principal elements of the eye are the subcellular structures of a photoreceptor, neurobiotin was incorporated efferently (retrogradely) from the cut end of an optic nerve. Neurobiotin spread into the rhabdomeric region as well as the cell body region (Fig. 1C-E), supporting the view that a single photoreceptor is composed of a rhabdomeric region, pigment layer, cell body layer, and optic nerve, as revealed by previous electron microscopic observations (Kataoka, 1975; Katagiri et al., 2001).

*Molecular phylogenetic analysis of arrestin*

We first searched for arrestin-like transcripts in *Limax*, and found a single arrestin-like transcript in our RNA-seq data of *Limax* (NCBI BioProject acc. no. PRJDB3972). Based on the partial cDNA sequence of the arrestin-like transcript of *Limax,* we obtained the nucleotide sequence information of the cDNA encompassing a putative full open reading frame using PCR-based method.

To confirm that there is only one arrestin gene in *Limax*, we searched for arrestin-like transcripts in the public nucleotide sequence database of National Center for Biotechnology Information (NCBI). We could detect only those 6 transcripts whose deduced amino acid sequences are highly similar (>86% identity) to that of *Limax*

β-arrestin in the "*Gastropoda*" subcategory of the non-redundant nucleotide collection using a TBLASTN program on the Web (https://blast.ncbi.nlm.nih.gov/Blast.cgi, Altschul et al., 1997, Genbank acc. nos. XM_013090298.1, XM_013212299.1, XM_013212298.1, XM_009058330.1, XM_013212300.1, XM_013090835.1). The deduced amino acid sequences in 4 of 6 transcripts contained the clathrin-binding domain, whereas the rest 2 lacked this domain because they were probably the partial sequences of the transcripts (XM_013212300.1 and XM_013090835.1). Therefore, *Limax* (and probably other gastropods) seemed to have only one arrestin gene.

A molecular phylogenetic tree was inferred using the amino acid sequences of various arrestin proteins, including both visual arrestin and β-arrestin from vertebrates and invertebrates (Fig. 2A). The tree was grouped into 4 clusters: vertebrate visual arrestin, vertebrate β-arrestin, invertebrate visual arrestin, and invertebrate β-arrestin. The arrestin of *Limax* was clearly grouped with invertebrate β-arrestin, which is consistent with the presence of clathrin-binding motif in its C-terminus (Fig. 2B). Yoshida et al. (2015) previously reported that several cephalopod mollusks (such as octopus and squids) possess visual arrestin lacking a clathrin-binding motif in its C-terminus, and these arrestin genes were grouped with a distinct cluster from that includes *Limax* arrestin (Fig. 2A).

*Expression of β-arrestin in the CNS of Limax*

To analyze the expression of β-arrestin protein in the CNS of *Limax*, we generated antiserum by immunizing a rabbit with recombinant β-arrestin protein, and the antibody was obtained by affinity-purification. The antibody gave rise to a strong immuno-reactive signal in the rhabdomeric region of the eye, and less intense signals in the remaining parts of the superior tentacle (Fig. 3A upper). The signals were almost diminished if the primary antibody was pre-incubated with recombinant β-arrestin protein (Fig. 3A lower) or if the primary antibody was omitted (Fig. S1). In the brain, there were no conspicuous signals. However, the weak immuno-reactive signals detected throughout the brain almost completely disappeared by pre-incubation of the primary antibody with the recombinant β-arrestin protein (Fig. 3B).

The antibody was also applicable to western blotting because it gave rise to bands with electrophoretic mobility identical to that of the full-length β-arrestin protein expressed in COS7 cells, although the detected bands exhibited a slightly larger molecular mass than that predicted from the amino acid sequence of β-arrestin (48.4 kDa, Fig. 3C).

Expression of β-arrestin mRNA was also examined by RT-PCR and fluorescence *in situ* hybridization. In RT-PCR, the band intensities had a trend similar to those in western blotting, where the band intensity was lower in the superior tentacle than those in the brain ganglia (Fig. 3C, D). Expression of β-arrestin mRNA was prominent in the cell body layer of the eye when an antisense probe was used in *in situ* hybridization, whereas no discernible signal was detected with the sense probe (Fig. 3E).

*Colocalization of β-arrestin and rhodopsin in the rhabdomere of the eye*

To see whether β-arrestin protein is localized to the rhabdomeric region of the retina, we generated a polyclonal antibody against the C-terminal peptide of rhodopsin (also called $G_q$-coupled opsin or rhabdomeric opsin), and visualized the rhabdomeric region by immunohistochemical staining of the rhodopsin. The specificity of the anti-rhodopsin antibody was confirmed by western blotting, where single bands of a slightly larger size than that of the predicted molecular size (60 kDa) were detected in the total lysate and crude membrane fraction of the superior tentacle, but not in the brain (Fig. 4A). The expression of rhodopsin mRNA was also confirmed in the cell body layer of the retina by *in situ* hybridization (Fig. 4B). The most prominent immuno-reactive signals of β-arrestin coincided with those of rhodopsin (Fig. 4C-H), and these corresponded to the rhabdomeric region of the retina (Fig. 1A, C).

*Light-dependent translocation of β-arrestin in the photosensory neuron*

Thus far, most of the studies on the light-dependent translocation of arrestin have been carried out for visual arrestin in the eyes of vertebrates and fruitflies (Broekhuyse et al., 1985; Philp et al., 1987; Kiselev et al., 2000; Nair et al., 2002; Lee et al., 2003). As an exception, however, it has been demonstrated that β-arrestin translocates in a light dependent manner in the pineal photosensory cell of the lamprey (Kawano-Yamashita et al., 2011). To examine whether β-arrestin in the slug's eye exhibits light-dependent subcellular translocation in photoreceptors, we analyzed the distribution of β-arrestin in the retina immunohistochemically. Illumination with 400 nm monochromatic light $(2.25 \times 10^{13}$ photons cm$^{-2}$sec$^{-1}$) for 3 h resulted in a change in the distribution of β-arrestin in the retina: a reduction in the cell body layer and an increase in the rhabdomeric region (Fig. 5A). The ratio of fluorescence intensity of the rhabdomeric region to that of the cell body layer increased over 3 h (Fig. 5B, $F_{(4,33)} = 6.505$, $P = 0.0006$), and began to increase as early as 30 min when compared to the dark-adapted state ($P = 0.0066$ by two-tailed Student's $t$-test).

We found that the retina of *Limax* exhibits a more robust ERG response to short wavelength light than to long wavelength light (Fig. 5C). The distribution of fluorescence was thus compared among the groups that were dark adapted (2 h), delivered short wavelength (400 nm) light, and long wavelength (600 nm) light. The light intensities were adjusted so that equivalent photon flux densities were delivered between 400 nm and 600 nm ($2.25 \times 10^{13}$ photons cm$^{-2}$sec$^{-1}$). As shown in Fig. 5D, no apparent increase of the fluorescence signals in the rhabdomere was evident in the long wavelength (600 nm) group. The ratio of fluorescence intensity of the rhabdomeric region to that of the cell body layer was larger in the short wavelength (400 nm) group than in the long wavelength (600 nm) group or in the dark adapted group (Fig. 5E, $F_{(2,21)} = 38.40$, $P < 0.0001$), whereas there was no difference between the dark adapted and the long wavelength groups ($P > 0.05$ by post-hoc Scheffé test). Moreover, the ratio increased moderately when more intense 600 nm light ($3.77 \times 10^{14}$ photons cm$^{-2}$sec$^{-1}$) was delivered for 2 h (Fig. S2, $F_{(2,22)} = 24.65$, $P < 0.0001$ among 400 nm at $2.25 \times 10^{13}$ photons cm$^{-2}$sec$^{-1}$, 600 nm at $2.25 \times 10^{13}$ photons cm$^{-2}$sec$^{-12}$, 600 nm at $3.77 \times 10^{14}$

photons cm$^{-2}$sec$^{-1}$).

Closer inspection of the thinner sections (6 μm-thick) revealed more detailed light-dependent subcellular re-distribution of β-arrestin. In the dark adapted eye, the immunoreactivity of β-arrestin exhibited a stripe-like pattern in a section intersecting near the center of the eye (Fig. 6A). The stripe-like pattern largely coincided with that of α-tubulin (Fig. 6A-E and S), which has been reportedly enriched in the AP of the rhabdomere (Fig. 1B, Kataoka, 1975; Martinez et al., 2000). Similarly, the dot-like distribution of β-arrestin was almost coincident with that of α-tubulin in a section crossing the AP of the rhabdomere (Fig. 6F-I and S). In contrast, the stripe-like pattern or dot-like distribution of β-arrestin became less evident in eyes illuminated with 400 nm monochromatic light for 2 h (Fig. 6J-Q), suggesting the re-distribution of β-arrestin into the microvilli of the rhabdomere in response to light (Fig. 6T).

Because visual arrestin has been known to be phosphorylated in a light-dependent manner in *Drosophila* and squid (Kahn and Matsumoto, 1997; Alloway and Dolph, 1999; Robinson et al., 2015), there is a possibility that the change in the immunoreactivity of β-arrestin is caused by the change in the binding affinity to the primary antibody due to phosphorylation. To test this possibility, the protein samples of the dark-adapted and light-adapted superior tentacles were blotted by anti-β-arrestin antibody in western blotting. There was no apparent mobility shift or change in band intensities between the two samples (Fig. 6R), suggesting that the light-dependent phosphorylation of β-arrestin, if any, does not affect the binding affinity to the polyclonal primary antibody used in the present study.

*β-arrestin as a marker of the optic nerve*

Because β-arrestin is enriched in the optic nerve as well as in the retina (Figs. 3A, 4C, 5D, Cross et al., 2015), we exploited the immunoreactivity of β-arrestin to visualize and trace the visual input pathway in *Limax*. Neurobiotin, a tracer molecule, was incorporated afferently from the cut end of the optic nerve, and the brain sections were stained with anti-β-arrestin antibody to see whether the commissural fiber that incorporated neurobiotin (Matsuo et al., 2014b) is a branch of the optic nerve. The

signal of neurobiotin colocalized with that of β-arrestin at the input region into the cerebral ganglia (Fig. 7A-C), whereas at the cerebral commissure, no prominent signal of β-arrestin was evident, and the neurobiotin signal did not overlap that of β-arrestin (Fig. 7D-F). Similarly, the immunoreactivity of FMRFamide, which has been demonstrated in the optic nerve of the pulmonate *Lymnaea* (Tuchina et al., 2012), also overlap with the signal of neurobiotin beneath the entry point into the brain (Fig. 7G-I), although this is less evident. However, these signals did not overlap each other at the cerebral commissure (Fig. 7J-M). Therefore, it is unlikely that the neurbiotin-stained commissural nerve is a branch of the optic nerve, but rather these commissural nerves may be a part of a neuron distinct from the photoreceptors.

*Monitoring of optic nerve regeneration following amputation*

Since an optic nerve can be visualized by immunostaining of β-arrestin, the spontaneous regeneration of an optic nerve was examined by immunohistochemistry in the coronal section of the brain at 14 days or 49 days following the amputation of the left superior tentacle. We have previously demonstrated that the olfactory nerves degenerate and retract at 15 days following tentacle amputation (Matsuo et al., 2010; Kobayashi et al., 2010), whereas olfactory function is restored at 31 days (Koga et al., 2016). We therefore expected that the signal of β-arrestin would be absent in the brain at 14 days whereas it would re-appear at 49 days. Indeed, we found that optic nerves could not be observed on the left side of the brain as a signal of β-arrestin immunoreactivity at 14 days (Fig. 8A-H), whereas they were detected on both sides of the brain at 49 days (Fig. 8I-P).

## DISCUSSION

In the present study, we found that β-arrestin is highly expressed in the retina of the *Limax* eye, and localized in the rhabdomeric region where photoreception takes place. Moreover, we found that β-arrestin translocates in response to light. Translocation into the microvilli of the rhabdomere would promote the rapid turnover of rhodopsin in a light environment, preventing saturation of a photosensory neuron's response (Arshavsky, 2003; Calvert et al., 2006). As far as we know, this is the first report on the light-dependent translocation of β-arrestin in invertebrate retina, suggesting the functional role of this molecule as a terminator of opsin signaling in the retina of those animals that lack visual arrestin. To demonstrate the role of β-arrestin more decisively, further investigation will be needed, such as an analysis of light-dependent binding of β-arrestin to the intracellular region of rhodopsin.

We demonstrated that β-arrestin translocated to the microvilli of the rhabdomere in the photoreceptor by illuminating it with short wavelength light (400 nm) to which the eye exhibits a robust ERG response. Translocation was not evident when long wavelength light (600 nm) was delivered at an equivalent photon flux density, whereas moderate translocation occurred when 600 nm light with higher photon flux density was delivered. Therefore, the translocation of β-arrestin is dependent on the activation of rhodopsin, consistent with a previous report that light-induced translocation of visual arrestin is absent in mice deficient in rhodopsin activation (Mendez et al., 2003).

We investigated the localization and light-dependent translocation of β-arrestin using a specific antibody that was raised against bacterially expressed β-arrestin protein. The specificity of the antibody was confirmed not only by preadsorption in immunohistochemistry but also by the observation that the expression pattern of β-arrestin mRNA (by RT-PCR, *in situ* hybridization) and β-arrestin protein (by immunohistochemistry and western blotting) were coincident (Fig. 3). The presence of β-arrestin throughout the brain tissue would reflect the fact that a single β-arrestin functions in terminating all G-protein signaling in gastropods. As neural tissues generally express higher levels of β-arrestin proteins than other non-neural tissues (Gainetdinov et al., 2004), relatively lower expression levels of β-arrestin in the superior

tentacle than in other brain areas (Fig. 3C, D) can be explained by the fact that the superior tentacle consists of both neural and non-neural tissues such as retractor muscles and epidermis.

We have previously observed that the fine commissural nerves between the bilateral cerebral ganglia incorporate neurobiotin delivered from the cut end of an optic nerve (Matsuo et al., 2014b). Similar results have also been reported in the marine gastropod *Aplysia* and the freshwater snail *Planorbarius* (Olson and Jacklet, 1985; Tuchina et al., 2011). Olson and Jacklet (1985) reported that the cell bodies of some neurons in the circumesophageal ganglia were labeled by horseradish peroxidase incorporated from the cut end of an optic nerve in *Aplysia*. These neurons were expected to be efferent neurons projecting to the eye. On the other hand, some of the labeled neuronal cell bodies in the study by Tuchina et al. (2011) may be secondary neurons receiving visual input from a photosensory neuron via gap junctions. It is because neurobiotin, but not horseradish peroxidase, passes through gap junctions, thereby potentially labeling all the neurons connected with optic nerves via electrical synapses. Because immunostaining of β-arrestin specifically labels optic nerves, it is possible to distinguish optic nerves entering into the brain from the efferent neurons or the secondary neurons connected via gap junctions.

The versatility of β-arrestin immunostaining would also be exerted to monitor the regeneration of an optic nerve during the recovery from the tentacle amputation or injury. Spontaneous recovery from tentacle amputation, such as cell proliferation and re-innervation, is a very complex and chaotic process in terrestrial pulmonates (Flores et al., 1992; Matsuo et al., 2010). Antibody against β-arrestin, therefore, will be a useful tool to trace the process of regeneration of optic nerves and re-innervation to the brain. Future studies will reveal the precise order of re-innervation of the visual pathway during spontaneous regeneration of the superior tentacle.

In most of the invertebrate's rhabdomere as well as lamprey pineal organ, the photoreceptor cells express bistable opsin, which photo-converts to a stable photoproduct that reverts to its original dark state by subsequent light absorption. In the lamprey pineal organ, these bistable opsins use β-arrestin instead of visual arrestin (Kawano-Yamashita et al., 2011; Koyanagi and Terakita, 2014). β-arrestin can

vigorously internalize activated opsin molecules by endocytosis that is mediated by a direct interaction with clathrin (Kawano-Yamashita et al., 2011). Internalization would be a useful strategy for a bistable opsin to retrieve its original dark state (Terakita et al., 2012; Koyanagi et al., 2017). On the other hand, the photoreceptor cells expressing bleaching opsins, whose photoproduct releases its retinal chromophore over time and decays (bleaches), such as vertebrate rhodopsin, have a visual arrestin lacking a clathrin-binding motif in its C-terminus. Therefore, it would be reasonable that gastropods have only β-arrestin (Fig. 2A), because they seem to use bistable rhabdomeric opsin like other mollusks (Koyanagi and Terakita, 2014).

However, insects and many of the cephalopods, whose visual pigments are also bistable, possess both visual arrestin and β-arrestin (Fig. 2A), and the expression levels of these mRNAs are comparable in the eye of the pygmy squid *Idiosepius* (Yoshida et al., 2015). What are the roles for these two arrestin proteins in the eye? Visual arrestin seems to play a major role in phototransduction signaling in the photosensory neurons of cephalopods: visual arrestin of the splendid squid *Loligo* binds activated rhodopsin, and functions in shutting off the rhodopsin signaling (Swardfager and Mitchell, 2007). Moreover, visual arrestin exhibits light-dependent translocation to the microvilli of the rhabdomere in *Drosophila* (Kiselev et al., 2000; Lee et al., 2003; Satoh et al., 2010). Therefore, visual arrestin might have taken over the role of β-arrestin in phototransduction during the course of the evolution of vertebrates and insects/cephalopods independently. β-arrestin, on the other hand, seems to still function in the internalization of the GPCRs other than opsins independently or in collaboration with visual arrestin in the photoreceptors of these animals (Deming et al., 2015). It is currently uncertain whether the emergence of visual arrestin precedes the divergence of the Lophotrochozoa (including cephalopods) and Ecdysozoa (including insects), although our molecular phylogenetic analysis supports the emergence of visual arrestin in the common ancestor of the two taxa (Fig. 2A).

Why insects and cephalopods gained visual arrestin during evolution despite their eyes express bistable opsin? The correlation between the possession of visual arrestin and the temporal/spatial resolution of the eye is of note. Vertebrates, cephalopods, and arthropods are the sole animal phyla that are equipped with an eye having the highest

temporal/spatial resolution and sensitivity in metazoan animals. Nilsson (2013) has argued that the eyes of the animals in these phyla have a well-developed light gathering system (lens), densely-arrayed photoreceptors, and innumerable number of membrane stacking of a photoreceptor, all of which enable the animal to perform daily tasks that require the visual system with high temporal/spatial resolution. Concomitantly, the performance of arrestin must be high in the photoreceptors in these animals at least to suffice the high temporal resolution. Indeed, the difference between the binding affinities to the active and inactive phosphorylated GPCRs is greater in visual arrestin than in β-arrestin in vertebrates (Celver et al,, 2002). This suggests a more efficient dissociation of visual arrestin from phosphorylated inactive opsins, probably allowing visual arrestin to do the next round of opsin signaling termination as well as rapid dephosphorylation of opsins by phosphatases for their reuse (Gurevich and Gurevich, 2015). It would be intriguing to see whether a similar kinetic difference exists between visual and β-arrestin in arthropods and cephalopods.

## ACKNOWLEDGEMENTS

## COMPETING INTERESTS

No conflicts of interest exist for any of the authors.

## FUNDING

# LIST OF ABBREVIATIONS

aa, amino acids

ANOVA, analysis of variance

AP, apical projection

CB, cell body layer

CC, cerebral commissure

CCD, cooled charge-coupled device

CG, cerebral ganglia

CNS, central nervous system

cRNA, complementary RNA

DAPI, 4',6-diamino-2-phenylindole

EDTA, ethylenediaminetetraacetic acid

ERG, electroretinogram

FMRFamide, Phe-Met-Arg-Phe-NH$_2$

GPCR, G protein-coupled receptor

GST, glutathione S-transferase

HEPES, 2-[4-(2-hydroxyethyl)-1-piperazineyl]ethanesulfonic acid

Mt, mitochondria

MV, microvilli

NHS, N-hydroxysuccinimide

ON, optic nerve

PBS, phosphate-buffered saline

PC, procerebrum

PL, pigment layer

RD, rhabdomeric region

RT-PCR, reverse transcription-polymerase chain reaction

SDS, sodium dodecyl sulfate

SE, standard error

SEG, subesophagealganglia

ST, superior tentacle

# REFERENCES

**Alloway P. G. and Dolph P. J.** (1999). A role for the light-dependent phosphorylation of visual arrestin. *Proc. Natl. Acad. Sci. USA* **96**, 6072-6077.

**Altschul A. F., Madden T. L., Schäffer A. A., Zhang J., Zhang Z., Miller W. and Lipman D. J.** (1997). Gapped BLAST and PSI-BLAST: a new generation of protein database search programs. *Nucleic Acid. Res.* **25**, 3389-3402.

**Arshavsky V. Y.** (2003). Protein translocation in photoreceptor light adaptation: a common theme in vertebrate and invertebrate vision. *Sci. STKE* **204**, PE43.

**Broekhuyse R. M., Tolhuizen E. F., Janssen A. P. and Winkens H. J.** (1985). Light induced shift and binding of S-antigen in retinal rods. *Curr. Eye Res.* **4**, 613-618.

**Calvert P. D., Strissel K. J., Schiesser W. E., Pugh E. N. Jr and Arshavsky V. Y.** (2006). Light-driven translocation of signaling proteins in vertebrate photoreceptors. *Trends Cell Biol.* **16**, 560-568.

**Celver J., Vishnivetskiy S. A. Chavkin C. and Gurevich V. V.** (2002). Conservation of the phosphate-sensitive elements in the arrestin family of proteins. *J. Biol. Chem.* **277**, 9043-9048.

**Cross S. D., Johnson A. A., Gilles B. J., Bachman L. A., Inoue T., Agata K., Marmorstein L. Y. and Marmorstein A.D.** (2015). Control of maintenance and regeneration of planarian eye by *ovo*. *Invest. Ophthamol. Vis. Sci.* **56**, 7604-7610.

**Deming J. D., Shin J. A., Lim K., Lee E. J., Van Craenenbroeck K. and Craft C. M.** (2015). Dopamine receptor D4 internalization requires a beta-arrestin and a visual arrestin. *Cell. Signal.* **27**, 20020-2013.

**Felsenstein J.** (1985). Confidence limits on phylogenies: an approach using the bootstrap. *Evolution* **39**, 783-791.

**Flores V., Brusco A., Scicolone G. and Saavedra J. P.** (1992). Serotonergic reinnervation of regenerating tentacular sensory organs in a pulmonate snail, *Cryptomphalus aspersa*. *Int. J. Dev. Neurosci.* **10**, 331-340.

**Fukunaga S., Matsuo R., Hoshino S. and Kirino Y.** (2006). Novel kruppel-like factor is induced by neuronal activity and sensory input in the central nervous system of the terrestrial slug *Limax valentianus*. *J. Neurobiol.* **66**, 169-181.

**Gainetdinov R. R., Premont R. T., Bohn L. M., Lefkowitz R. J. and Caron M. G.** (2004). Desensitization of G-protein coupled receptors and neuronal functions. *Ann. Rev. Neurosci.* **27**, 107-144.

**Gurevich E. V. and Gurevich V. V.** (2006). Arrestins: ubiquitous regulators of cellular signaling pathways. *Genome Biol.* **7**, 236.

**Gurevich E. V. and Gurevich V. V.** (2015). Arrestins: Critical players in trafficking of many GPCRs. *Prog. Mol. Biol. Transl. Sci.* **132**, 1-13.

**Hampson E. C., Vaney D. I. and Weiler R.** (1992). Dopaminergic modulation of gap junction permeability between amacrine cells in mammalian retina. *J. Neurosci.* **12**, 4911-4922.

**Kahn E. S. and Matsumoto H.** (1997). Calcium/calmodulin-dependent kinase II phosphorylates *Drosophila* visual arrestin. *J. Neurochem.* **68**, 169-175.

**Katoh K., Misawa K., Kuma K. and Miyata T.** (2002). MAFFT: a novel method for rapid multiple sequence alignment based on fast Fourier transform. *Nucleic Acids Res.* **30**, 3059-3066.

**Katagiri N., Terakita A., Shichida Y. and Katagiri Y.** (2001). Demonstration of a rhodopsin-retinochrome system in the stalk eye of a marine gastropod, *Onchidium*, by immunohistochemistry. *J. Comp. Neurol.* **433**, 380-389.

**Kataoka S.** (1975). Fine structure of the retina of a slug, *Limax flavus* L. *Vision Res.* **15**, 681-686.

**Kawano-Yamashita E., Koyanagi M., Schichida Y., Oishi T., Tamotsu S. and Terakita A.** (2011). Beta-arrestin functionally regulates the non-bleaching pigment in lamprey pineal. *PLoS one* **6**, e16402.

**Kiselev A., Socolich M., Vinos J., Hardy R. W., Zuker C. S. and Ranganathan R.** (2000). A molecular pathway for light-dependent photoreceptor apoptosis in *Drosophila*. *Neuron* **28**, 139-152.

**Kobayashi S., Hattori M., Elekes K., Ito E. and Matsuo R.** (2010). FMRFamide regulates oscillatory activity of the olfactory center in the slug. *Eur. J. Neurosci.* **32**, 1180-1192.

**Koga Y., Matsuo Y. and Matsuo R.** (2016). Olfactory memory storage and/or retrieval requires the presence of the exact tentacle used during memory acquisition in the terrestrial slug *Limax*. *Zool. Sci.* **33**, 78-82.

**Koyanagi M., Kawano E., Kinugawa Y., Oishi T., Shichida Y., Tamotsu S. and Terakita A.** (2004). Bistable UV pigment in the lamprey pineal. *Proc. Natl. Acad. Sci. USA* **101**, 6687-6691.

**Koyanagi M. and Terakita A.** (2014). Diversity of animal opsin-based pigments and their optogenetic potential. *Biochem. Biophys. Acta* **1873**, 710-716.

**Koyanagi M., Kawano-Yamashita E., Wada S. and Terakita A.** (2017). Vertebrate bistable parapinopsin: implications for emergence of visual signaling and neofunctionalization of non-visual pigment. *Front. Ecol. Evol.* **5**, article 23.

**Land, M. F. and Nilsson, D. E.** (2012). *Animal Eyes.* Oxford, UK: Oxford University Press.

**Lee S. J., Xu H., Kang L. W., Amzel L. M. and Montell C.** (2003). Light adaptation through phosphoinositide-regulated translocation of *Drosophila* visual arrestin. *Neuron* **39**, 121-132.

**Martinez J. M., Elfarissi H., De Velasco B., Ochoa G. H., Miller A. M., Clark Y. M., Matsumoto B. and Robles L. J.** (2000). Distribution of tubulin, kinesin, and dynein in light- and dark-adapted octopus retinas. *Vis. Neurosci.* **17**, 127-138.

**Matsuo R., Asada A., Fujitani K. and Inokuchi K.** (2001). *LIRF*, a gene induced during hippocampal long-term potentiation as an immediate-early gene, encodes a novel RING finger protein. *Biochem. Biophys. Res. Commun.* **289**, 479-484.

**Matsuo R., Kobayashi S., Tanaka Y. and Ito E.** (2010). Effects of tentacular amputation and regeneration on the morphology and activity of the olfactory center of the terrestrial slug *Limax valentianus*. *J. Exp. Biol.* **213**, 3144-3149.

**Matsuo R., Kobayashi S., Wakiya K., Yamagishi M., Fukuoka M. and Ito E.** (2014a). The cholinergic system in the olfactory center of the terrestrial slug *Limax*. *J. Comp. Neurol.* **522**, 2951-2966.

**Matsuo Y., Uozumi N. and Matsuo R.** (2014b). Photo-trapotaxis based on projection throught the cerebral commissure in the terrestrial slug *Limax*. *J. Comp. Physiol. A* **200**, 1023-1032.

**Mendez A., Lem J., Simon M. and Chen J.** (2003). Light-dependent translocation of arrestin in the absence of rhodopsin phosphorylation and transducin signaling. *J. Neurosci.* **23**, 3124-3129.

**Nair K. S., Balasubramanian N. and Slepak V. Z.** (2002). Signal-dependent translocation of transducin, RGS9-1-Gβ5L complex, and arrestin to detergent-resistent membrane rafts in photoreceptors. *Curr. Biol.* **12**, 421-425.

**Nilsson D. E.** (2013). Eye evolution and its functional basis. *Vis. Neurosci.* **30**, 5-20.

**Olson L. M. and Jacklet J. W.** (1985). The circadian pacemaker in the *Aplysia* eye sends axons throughout the central nervous system. *J. Neurosci.* **12**, 3214-3227.

**Philp N. J., Chang W. and Long K.** (1987). Light-stimulated protein movement in rod photoreceptor cells of the rat retina. *FEBS Lett.* **225**, 127-132.

**Robinson K. A., Ou W. L., Guan X., Sugamori K. S., Bandyopadhyay A., Ernst O. P. and Mitchell J.** (2015). The effect of phosphorylation on arrestin-rhodopsin interaction in te squid visual system. *J. Neurochem.* **135**, 1129-1139.

**Saitou N. and Nei M.** (1987). The neighbor-joining method: a new method for reconstructing phylogenetic trees. *Mol. Biol. Evol.* **4**, 406-425.

**Satoh A. K., Xia H., Yan L., Liu C. H., Hardie R. C. and Ready D. F.** (2010). Arrestin translocation is stoichiometric to rhodopsin isomerization and accelerated by phototransduction in *Drosophila* photoreceptors. *Neuron* **67**, 997-1008.

**Swardfager W. and Mitchell J.** (2007). Purification of visual arrestin from squid photoreceptors and characterization of arrestin interaction with rhodopsin and rhodopsin kinase. *J. Neurochem.* **101**, 223-231.

**Terakita A., Kawano-Yamashita E. and Koyanagi M.** (2012). Evolution and diversity of opsins. *WIREs Membr. Transp. Signal.* **1**, 104-111.

**Tuchina O. P., Zhukov V. V. and Meyer-Rochow V. B.** (2011). Afferent and efferent pathways in the visual system of the freshwater snail *Planorbarius corneus*. *Zool. Res.* **32**, 403-420.

**Tuchina O. P., Zhukov V. V. and Meyer-Rochow V. B.** (2012). Distribution of serotonin an FMRF-amide in the brain of *Lymnaea stagnalis* with respect to the visual system. *Zool. Res.* **33**, E1-E12.

**Yamagishi M., Ito E. and Matsuo R.** (2008). Redundancy of olfactory sensory pathways for odor-aversion memory in the terrestrial slug *Limax valentianus*. *J. Exp. Biol.* **211**, 1841-1949.

**Yamagishi M., Ito E. and Matsuo R.** (2012). Whole genome amplification in large neurons of the terrestrial slug *Limax*. *J. Neurochem.* **122**, 727-737.

**Yoshida M. A., Ogura A., Ikeo K., Shigeno S., Moritaki T., Winters G. C., Kohn A. B. and Moroz L. L.** (2015). Molecular evidence for convergence and parallelism in evolution of complex brains of cephalopod molluscs: insights from visual systems. *Integr. Comp. Biol.* **55**, 1070-1083.

**Figures**
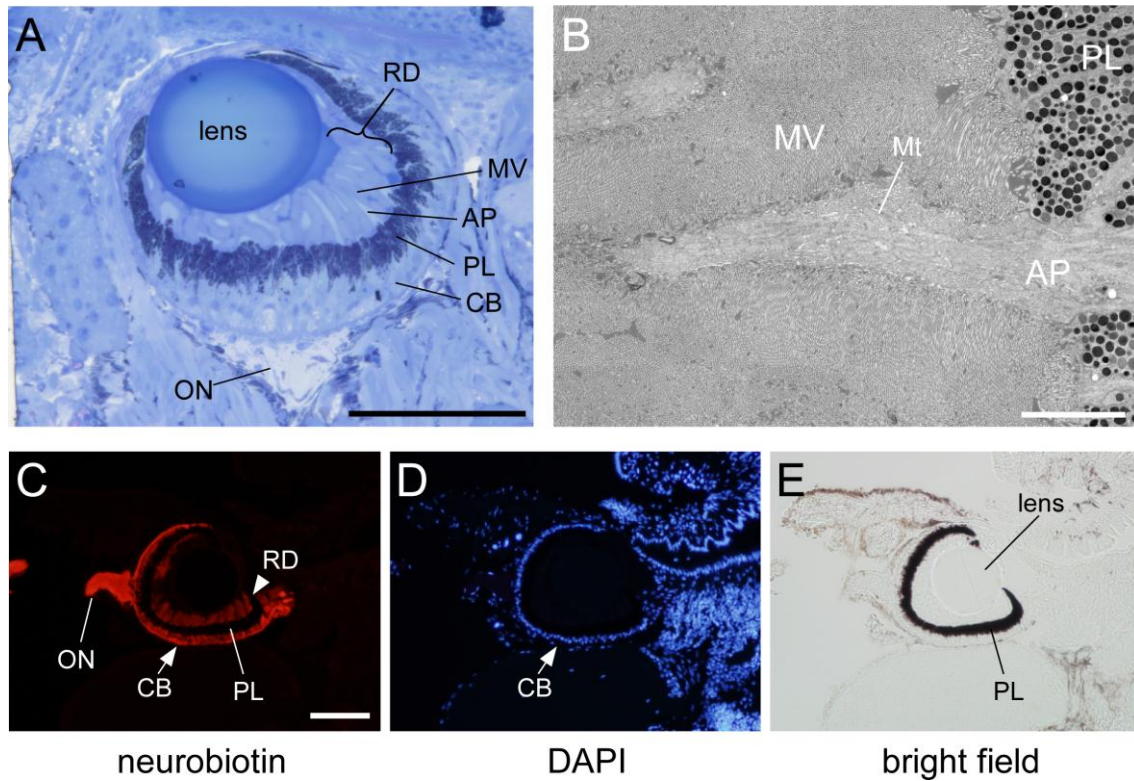


Figure 1 Structure of the eye of *Limax*. (A) A toluidine-blue stained semithin section of an eye. (B) A photograph of the rhabdomeric region by electron microscopy. Innumerable numbers of microvilli are coming out from the apical projection of a photoreceptor. Numerous mitochondria are visible in the apical projection. (C) Neurobiotin efferently incorporated from the cut end of an optic nerve. (D) A fluorescence image of DAPI of (C). (E) A bright field image of (C). Scale bars: 100 μm for (A, C) and 5 μm for (B). RD, rhabdomeric layer; MV, microvilli; PL, pigment layer; AP, apical projection; Mt, mitochondria; CB, cell body layer; ON, optic nerve.
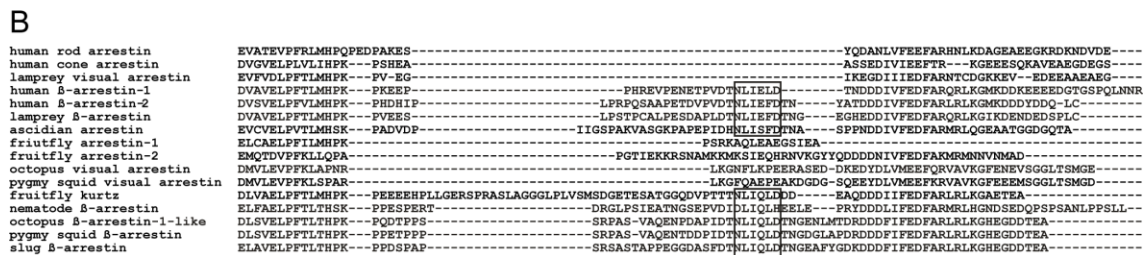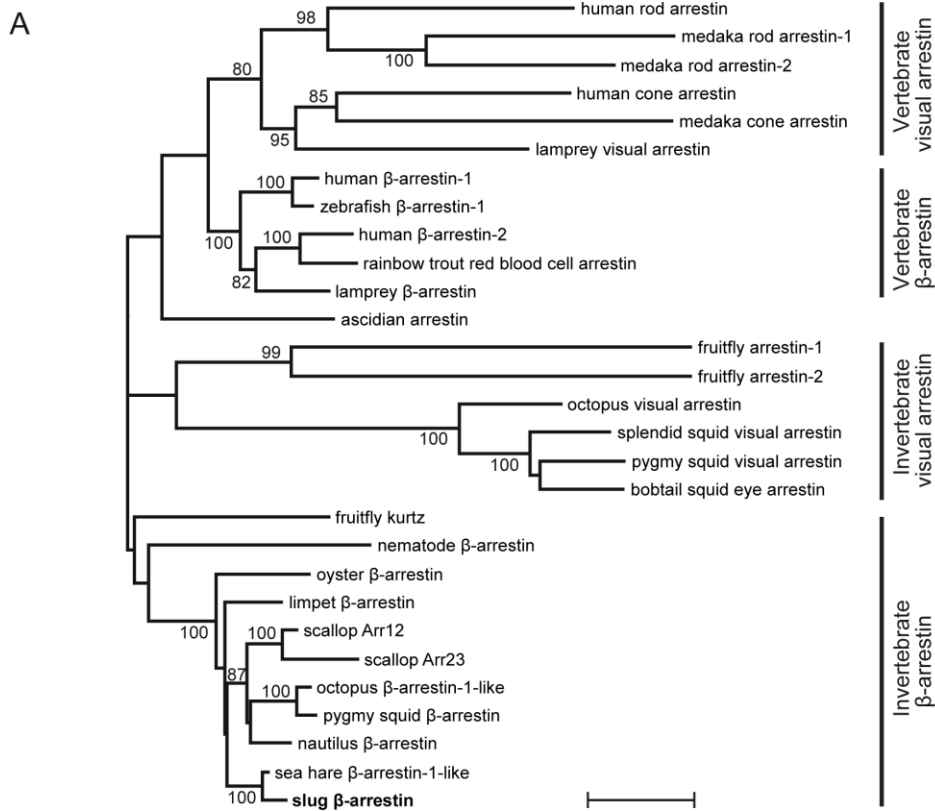
Figure 2  Phylogenetic position of *Limax* (slug) β-arrestin. (A) An unrooted molecular phylogenetic tree of the arrestin family. Invertebrate arrestins are divided into two groups and *Limax* β-arrestin was classified into the invertebrate β-arrestin group, but not the visual arrestin group. The bootstrap probabilities (≥80%) are indicated at each branch node. Scale bar, 0.1 substitutions per site. (B) Comparison of the amino acid sequences of the C-terminal region of vertebrate and invertebrate arrestins. A clathrin-binding motif (boxed) is conserved in both vertebrate and invertebrate β-arrestin including *Limax* β-arrestin.

A

eye

eye
(preadsorbed)

DAPI

bright field

B

brain

brain
(preadsorbed)

A
L — R
P

D
L — R
V

CG

SEG

C

CG SEG ST COS7 COS7-arrestin

kDa

100 —
75 —
63 —
48 —

35 —

25 —

α-tubulin

D

CG SEG ST

arrestin

18S rRNA

E

antisense

sense

DAPI

bright
field
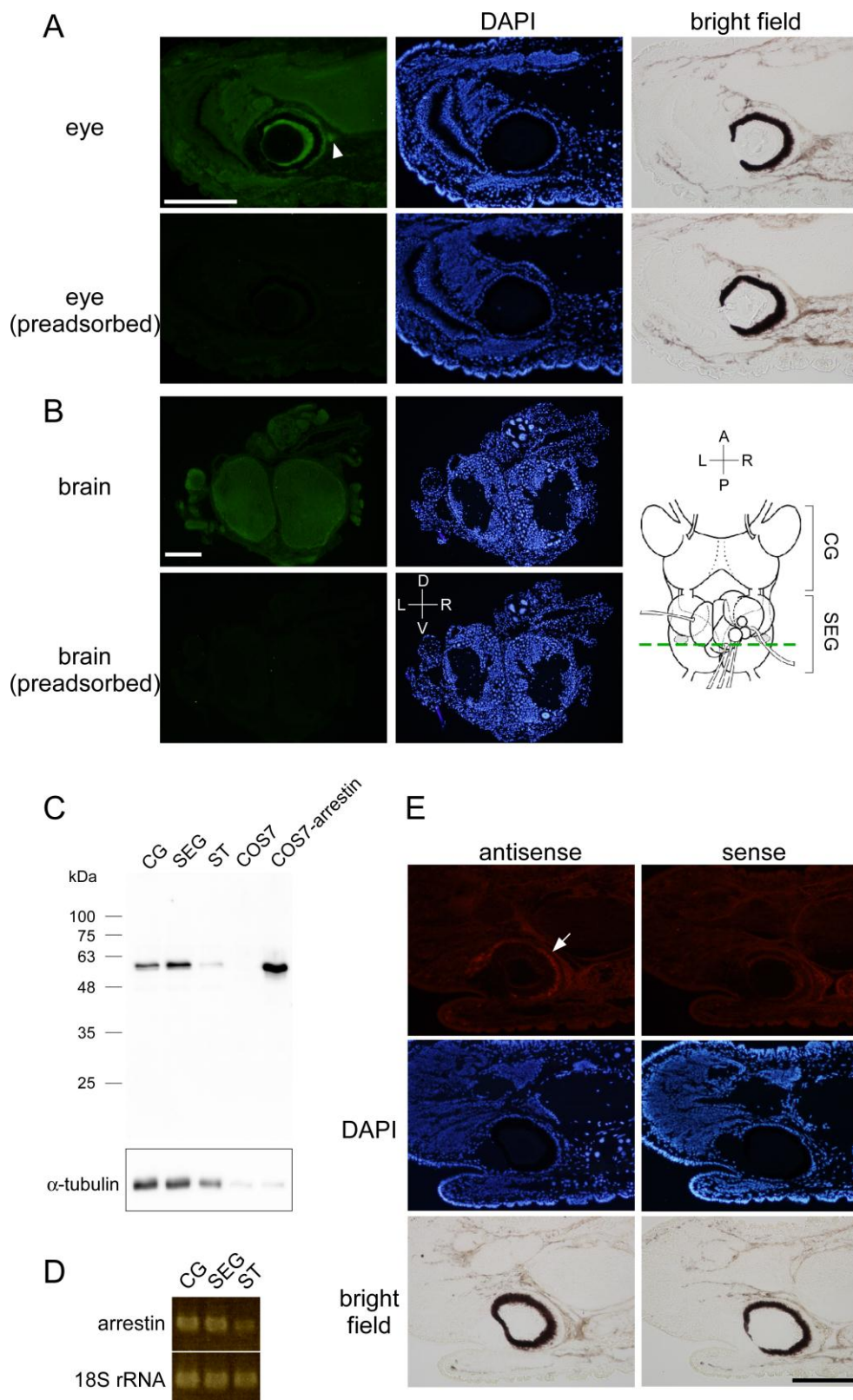
Figure 3 Expression of β-arrestin in the eye and brain. (A) Immunohistochemical staining of β-arrestin in the superior tentacle. Immunoreactivity was almost diminished by preadsorption of the primary antibody with recombinant β-arrestin protein. The images of DAPI staining (middle) and bright field (right) show the cell nuclei and the pigment layer, respectively. A white arrowhead indicates the proximal end of an optic nerve. (B) Immunohistochemical staining of β-arrestin in the brain. Immunoreactivity almost disappeared by preadsorption of the primary antibody with recombinant β-arrestin protein. The images of DAPI staining show the distribution of cell nuclei. The cartoon on the right shows the cutting plane of the brain section (dorsal view). (C) Western blotting of β-arrestin. Below is the blot of α-tubulin to demonstrate the equivalence of the protein amount (3 μg) loaded. Note the band intensities of α-tubulin are different between the brain homogenates (left 3 lanes) and COS7 lysates (right 2 lanes), possibly because of the difference in the animal species (the slug or African green monkey) and the tissue type. (D) RT-PCR of β-arrestin in different parts of the CNS. Amplicons of 18S rRNA serve as an internal control for the equivalence of the cDNA templates used. (E) Fluorescence *in situ* hybridization of β-arrestin in the eye. A white arrow indicates positive signals in the cell body layer of the retina. The images of DAPI staining (middle) and bright field (lower) show the locations of the cell bodies and the pigment granule layer, respectively. Scale bars: 200 μm. CG, cerebral ganglia; SEG, subesophageal ganglia; ST, superior tentacle; D, dorsal; V, ventral; A, anterior; P, posterior; R, right; L, left.
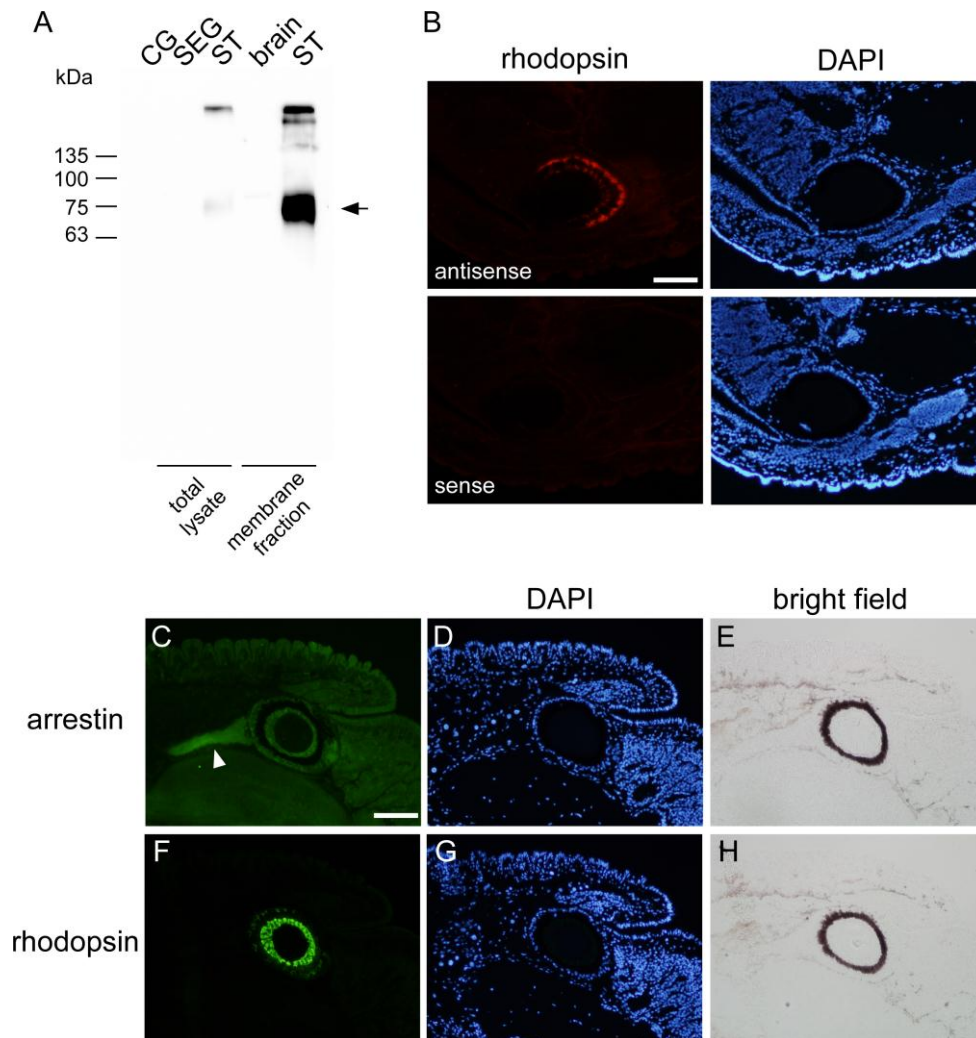
Figure 4   Expression of β-arrestin and rhodopsin in the rhabdomere. (A) Western blotting of rhodopsin. Five μg protein was loaded and electrophoresed. An arrow indicates the bands with the mobility slightly larger than predicted size (60 kDa). (B) Fluorescence *in situ* hybridization of rhodopsin in the eye. The images of DAPI staining (right) show the location of the cell body layer. (C-H) Serial sections (6 μm-thick) of the superior tentacle stained with anti-β-arrestin (C) and anti-rhodopsin (F) antibodies. A white arrowhead indicates an optic nerve. (D) and (G) are the images of DAPI staining. (E) and (H) are the bright field images. Scale bars: 100 μm. CG, cerebral ganglia; SEG, subesophageal ganglia; ST, superior tentacle.
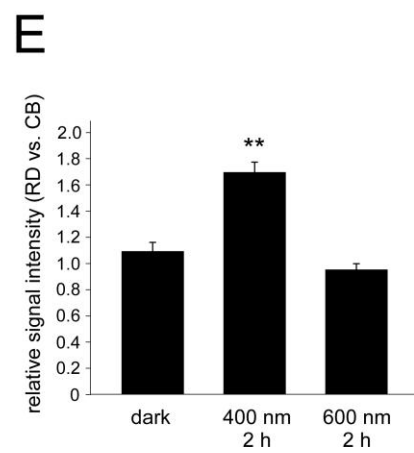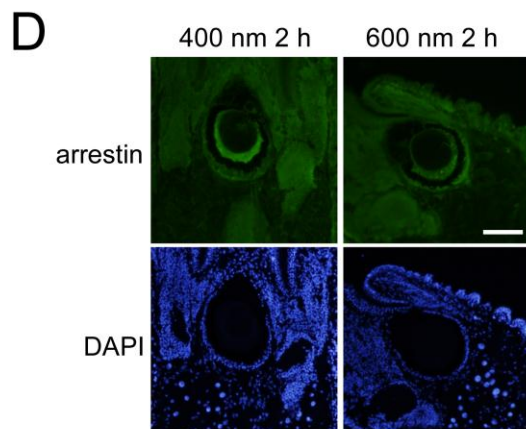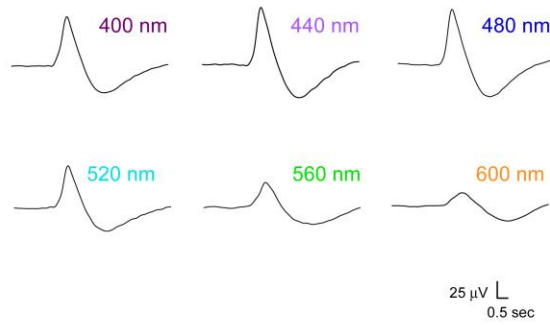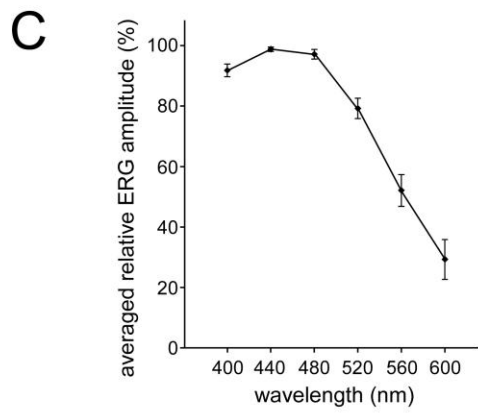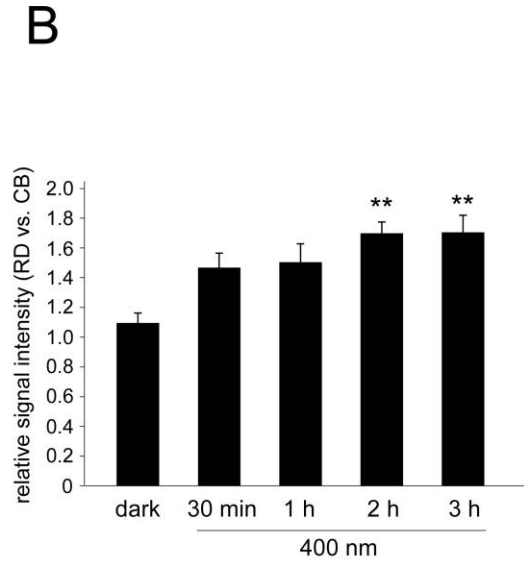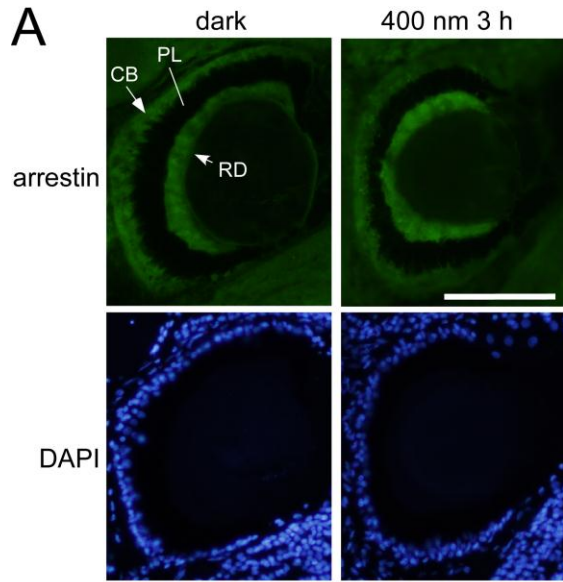
Figure 5 Light-dependent translocation of β-arrestin in the retina. (A) Immunohistochemical staining of β-arrestin in the superior tentacle kept in dark for 2 h or illuminated with light (400 nm) for 3 h after being kept in the dark for 2 h. (B) Change in the relative intensities of β-arrestin immunoreactivity over time. The superior tentacles were kept in the dark for 2 h, followed by illumination (400 nm) for 30 min, 1 h, 2 h, or 3 h. Error bars indicate ±SE of the mean among 6 − 8 independent samples. **$P < 0.01$ vs. dark (2 h) by post hoc Scheffé tests. (C) The wavelength dependence of ERG amplitude. Error bars: ±SE (n = 8). Representative ERG responses are shown to the right. (D, E) Illumination with 600 nm light did not elicit translocation of β-arrestin. Error bars: ±SE (n = 8). **$P < 0.01$ vs. dark (2 h) and vs. 600 nm group by post hoc Scheffé tests. Scale bars: 100 μm. CB, cell body layer; PL, pigment layer; RD, rhabdomeric layer.
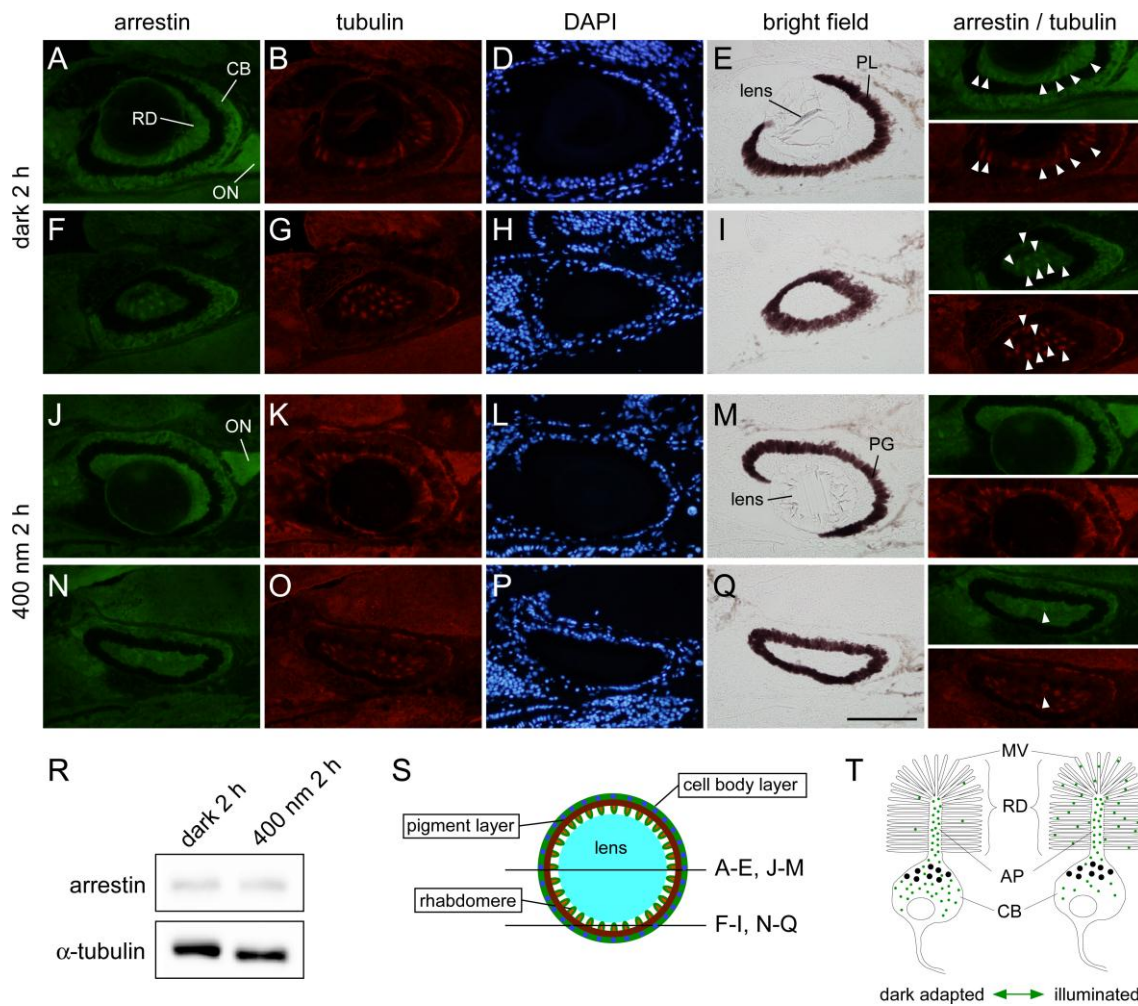
Figure 6  β-arrestin immunoreactive signals dispersed out from the apical projection of rhabdomere during illumination with 400 nm light. (A-I) Dark-adapted (2 h) eyes. (J-Q) Eyes illuminated with 400 nm light (2 h) following 2 h dark adaptation. White arrowheads in the right panels indicate the colocalization of β-arrestin and α-tubulin. (R) Western blotting of β-arrestin showing the absence of apparent change in the molecular mass or immunoreactivity after illumination. The same amounts (7.5 μg) of protein were loaded on the two lanes. (S) A schema showing the cutting planes of the sections. (T) A schema explaining the light-dependent redistribution of β-arrestin. Scale bar: 100 μm. RD, rhabdomeric layer; CB, cell body layer; PL, pigment layer; ON, optic nerve; AP, apical projection; MV, microvilli.
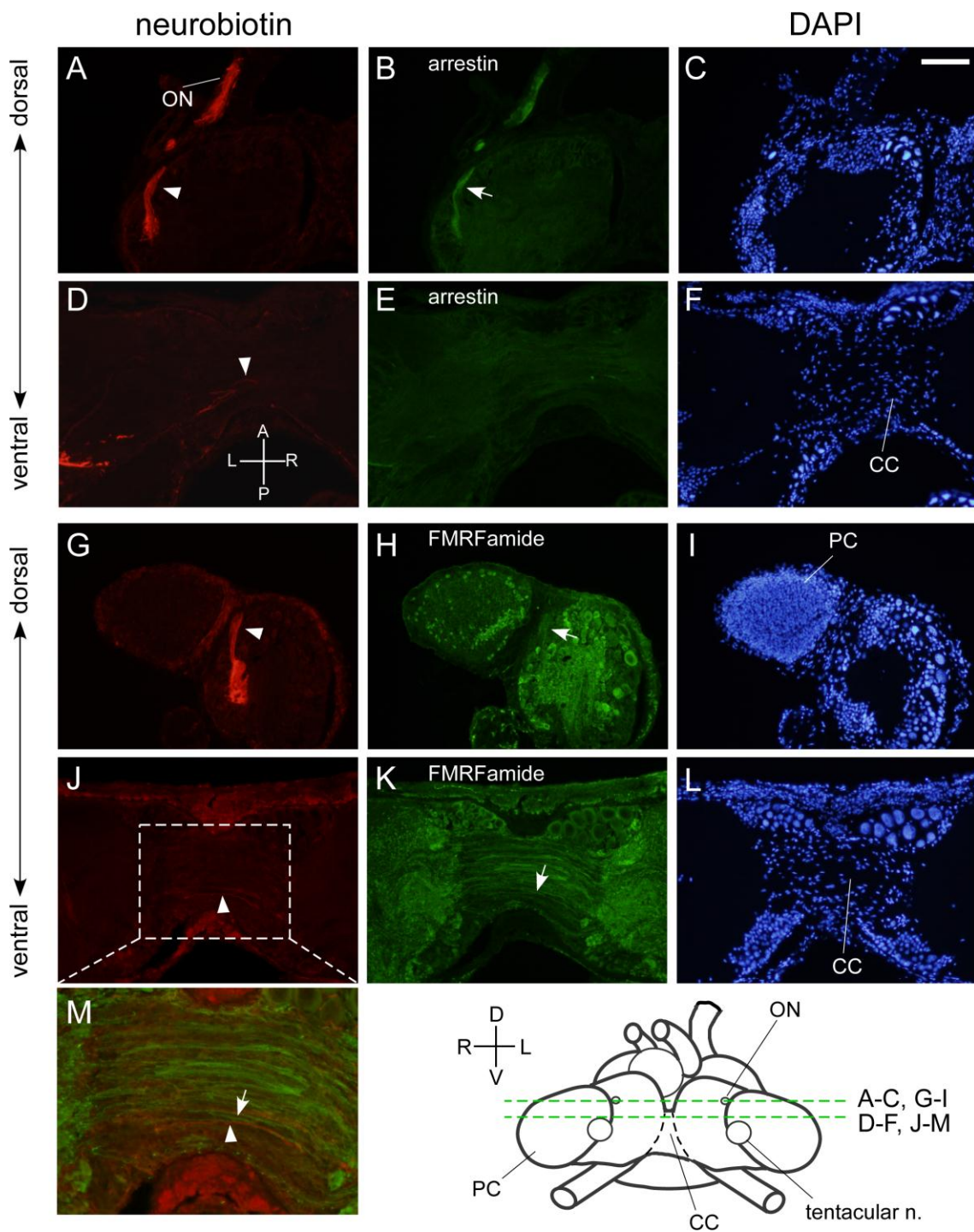
Figure 7    Visualization of the optic nerve entering into the brain by immunohistochemical staining of β-arrestin. (A, D) Tracing of visual input pathway by neurobiotin (arrowhead) incorporated from the cut end of the left optic nerve. (B, E) Immunostaining of β-arrestin (arrow) of the same sections of (A, D). (C, F) Fluorescence images of DAPI of (A, D). (G, J) Tracing of visual input pathway by neurobiotin incorporated from the cut end of the left optic nerve. (H, K) Immunostaining of FMRFamide of the same sections as respective (G, J). (I, L) Fluorescence images of DAPI of (G, J). (M) A merged image of (J) and (K), corresponding to the region circumscribed with a broken line in (J). An arrowhead and an arrow indicate the signals of neurobiotin and FMRFamide, respectively. A schema at the bottom shows the cutting planes of the sections drawn on the cartoon of the brain (anterior view). Note that the background red fluorescence is higher in the sections of the brain fixed with Bouin fixative (G, J, M) than those of the brain fixed with paraformaldehyde (A, D). CC, cerebral commissure; ON, optic nerve; PC, procerebrum. Scale bar: 100 μm. A, anterior; P, posterior; D, dorsal; V, ventral; R, right; L, left.
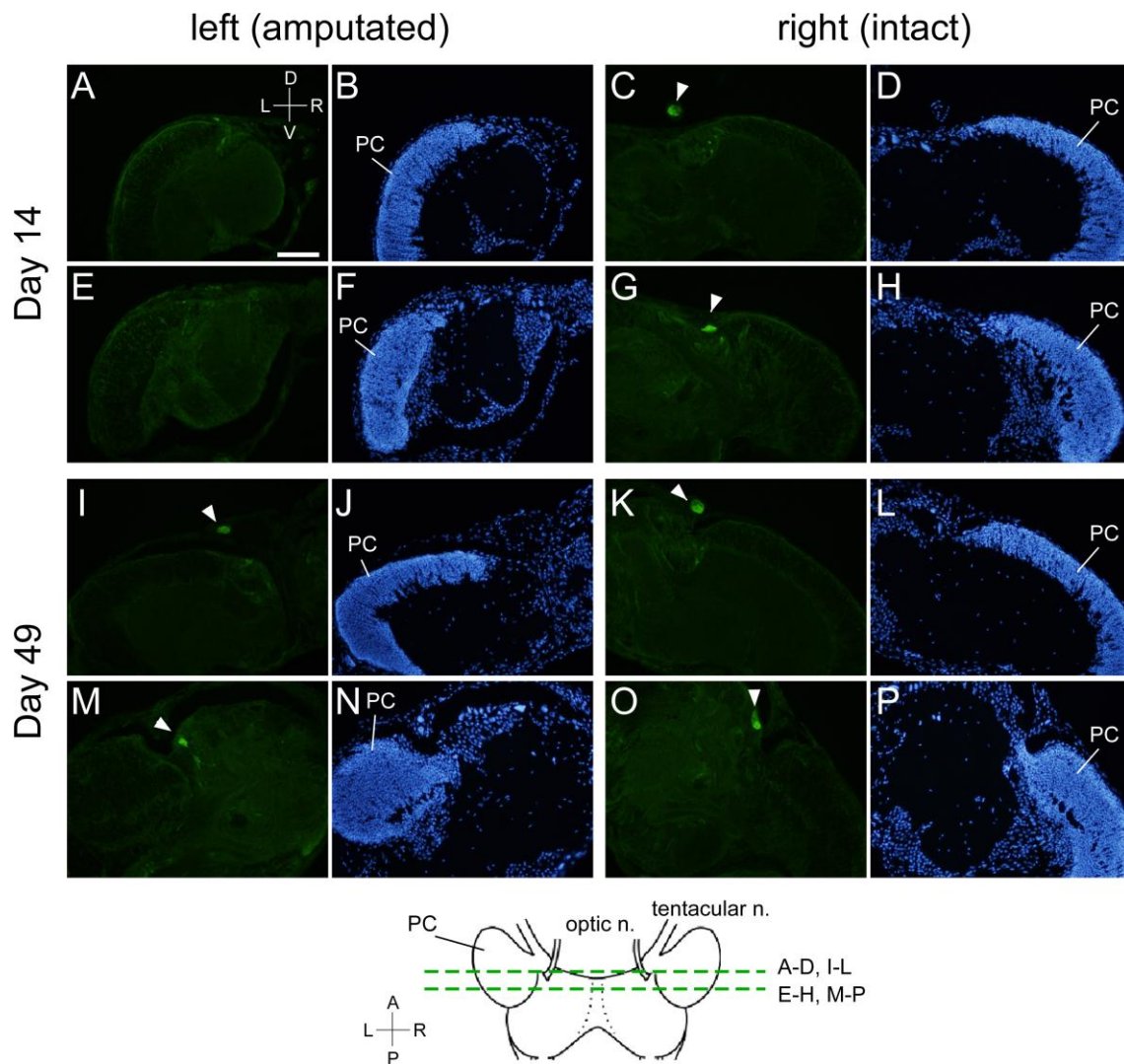
Figure 8    Regeneration of an optic nerve visualized by immunostaining of β-arrestin. Immunostaining of β-arrestin in the coronal sections of the cerebral ganglia 14 days (A-H) or 49 days (I-P) after the surgical amputation of the left superior tentacle. (B, D, F, H, J, L, N, P) are the fluorescence images of DAPI of corresponding images to their left. White arrowheads indicate the β-arrestin signals in the optic nerve. A schema at the bottom shows the cutting planes of the sections. Scale bar: 200 μm. PC, procerebrum. D, dorsal; V, ventral; A, anterior; P, posterior; R, right; L, left.
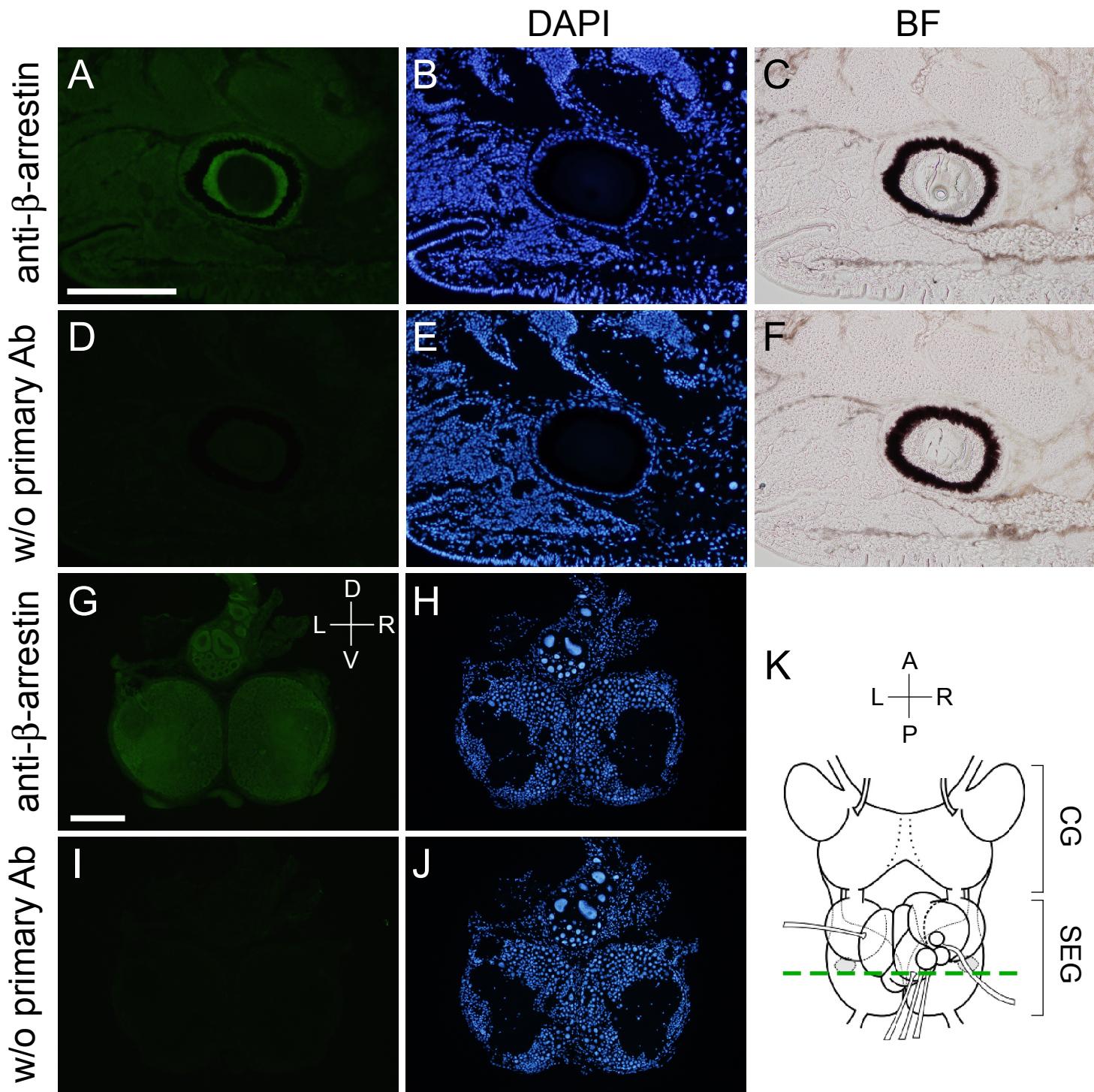
**Figure S1** Specificity of anti β-arrestin antibody.

Immuno-positive signals of β-arrestin (A, G) were absent if the primary antibody was omitted (D, I), suggesting that the secondary antibody does not bind to the section in a non-specific manner. (B, E, H, I) are the fluorescence images of DAPI of (A, D, G, I). (C, F) are the bright field images of (A, D). (K) A schema showing the cutting plane of the brain section of (G-J). Scale bars: 200 μm. CG, cerebral ganglia; SEG, subesophageal ganglia; A, anterior; P, posterior; R, right; L, left; D, dorsal; V, ventral.
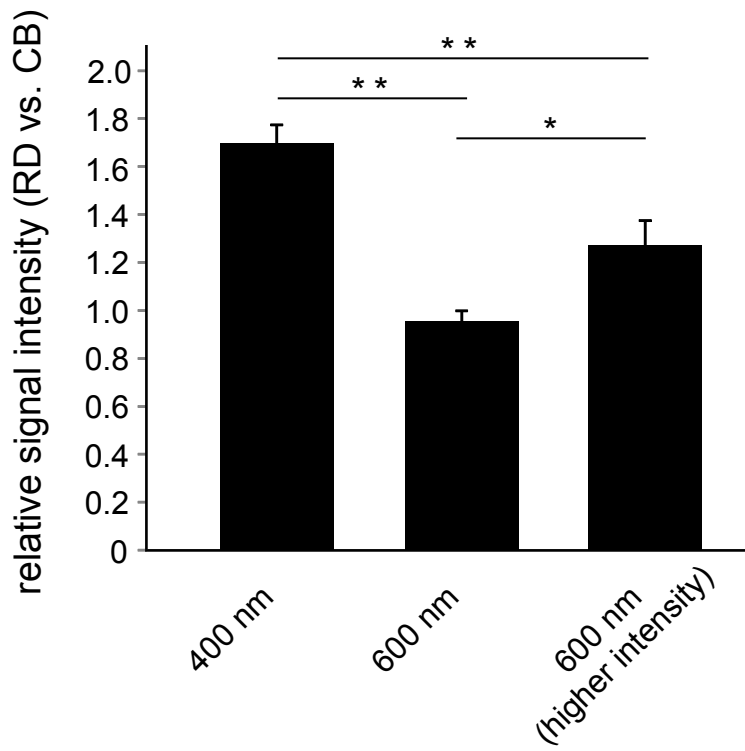
Figure S2 Illumination with 600 nm light with higher intensity ($3.77 \times 10^{14}$ photons cm$^{-2}$sec$^{-1}$) moderately elicited the translocation of $\beta$-arrestin.
The superior tentacles were kept in the dark for 2 h, followed by illumination (400 nm or 600 nm) for 2 h. The data for 400 nm ($2.25 \times 10^{13}$ photons cm$^{-2}$sec$^{-1}$) and 600 nm ($2.25 \times 10^{13}$ photons cm$^{-2}$sec$^{-1}$) are reproduced from Fig. 5E. Error bars indicate $\pm$SE of the mean among 7 - 8 independent samples. **$P < 0.01$, *$P < 0.05$ by post hoc Scheffe tests.